Journal of Biomolecular NMR, **17:** 187–194, 2000.
KLUWER/ESCOM

Rapid fold and structure determination of the archaeal translation elongation factor 1β from *Methanobacterium thermoautotrophicum*

Guennadi Kozlov[a,e], Irena Ekiel[b,e], Natalia Beglova[a,e,*], Adelinda Yee[c,d], Akil Dharamsi[c], Asaph Engel[c], Nadeem Siddiqui[a,e], Andrew Nong[a,e] & Kalle Gehring[a,e,**]
[a]*McGill University, Department of Biochemistry, McIntyre Medical Science Building, 3655 Promenade Sir William Osler, Montréal, PQ, Canada H3G 1Y6;* [b]*Biomolecular NMR Group, Sector of Pharmaceutical Biotechnology, Biotechnology Research Institute, National Research Council of Canada, 6100 Royalmount Ave., Montréal, PQ, Canada H4P 2R2;* [c]*Department of Medical Biophysics, University of Toronto, and* [d]*Ontario Cancer Institute, 610 University Ave., Rm 7-714, Toronto, ON, Canada M5G 2M9;* [e]*Montreal Joint Centre for Structural Biology*

Received 3 March 2000; Accepted 8 May 2000

Key words: archaebacteria, elongation factor, guanine exchange factor, structural genomics, tertiary fold

Abstract

The tertiary fold of the elongation factor, aEF-1β, from *Methanobacterium thermoautotrophicum* was determined in a high-throughput fashion using a minimal set of NMR experiments. NMR secondary structure prediction, deuterium exchange experiments and the analysis of chemical shift perturbations were combined to identify the protein fold as an alpha-beta sandwich typical of many RNA binding proteins including EF-G. Following resolution of the tertiary fold, a high resolution structure of aEF-1β was determined using heteronuclear and homonuclear NMR experiments and a semi-automated NOESY assignment strategy. Analysis of the aEF-1β structure revealed close similarity to its human analogue, eEF-1β. In agreement with studies on EF-Ts and human EF-1β, a functional mechanism for nucleotide exchange is proposed wherein Phe46 on an exposed loop acts as a lever to eject GDP from the associated elongation factor G-protein, aEF-1α. aEF-1β was also found to bind calcium in the groove between helix α2 and strand β4. This novel feature was not observed previously and may serve a structural function related to protein stability or may play a functional role in archaeal protein translation.

Abbreviations: aEF-1β, archaeal translation elongation factor 1 beta; aEF-1α, archaeal translation elongation factor 1 alpha; eEF-1β, eukaryotic translation elongation factor 1 beta.

Introduction

The exponential growth in genomic studies has produced an enormous amount of information about DNA and protein sequences. This promises to revolutionize biology, providing new perspectives and tools for drug development and understanding diseases. Through homology modeling, roughly a third of newly discovered protein coding sequences can be assigned functions; structural studies can significantly enhance this process through the application of high-throughput structure determination. The maturation of modern X-ray and NMR techniques has led to the development of the field of structural genomics, which promises '100 000 protein structures for the biologist' (Sali, 1998).

Current estimates suggest that 85% to 90% of newly determined proteins have a previously known fold (Berman et al., 2000; Brenner and Levitt, 2000). While protein prediction methods can predict many of these structures, a significant percentage will require structure determination. Since newly discovered genes highly outnumber the current capabilities of structural

*Present address: Dept. of Pathology, Brigham and Women's Hospital, Thorn 528A, Harvard Medical School, 75 Francis St., Boston, MA 02115, U.S.A.
**To whom correspondence should be addressed. E-mail: Kalle.Gehring@bri.nrc.ca

studies, a sensible compromise is to determine the minimal number of structures which define functional protein families. Especially efficient sampling can be attained by determining homologous structures from organisms belonging to different kingdoms. When similar, these proteins define the range of structures in the functional family.

This approach was applied towards the archaeal elongation factor, aEF-1β, from *Methanobacterium thermoautotrophicum*. The structure of its human homologue, eEF-1β, was published recently (Perez et al., 1999) and the structure of the bacterial homologue, EF-Ts, is known (Jiang et al., 1996; Kawashima et al., 1996; Wang et al., 1997). EF-1β is a guanine nucleotide exchange factor (GEF) and belongs to a class of accessory proteins involved in the translation of mRNA into proteins. These GEFs catalyze GDP/GTP exchange in translation factor G-proteins. In archaebacteria, aEF-1β releases GDP from the elongation factor, aEF-1α (Arcari et al., 1994, 1995; Masullo et al., 1994; Raimo et al., 1996). At present, there are relatively few structures of G-protein/GEF complexes: EF-Tu/EF-Ts (Kawashima et al., 1996; Wang et al., 1997), Ras/Sos1-CDC25 domain (Boriack et al., 1998), and ARF1/Gea2-Sec7 domain (Cherfils et al., 1998). While the structures of G-proteins are relatively conserved, the exchange proteins have distinct structures suggesting the possibility of different mechanisms of nucleotide exchange (for a review, see Sprang and Coleman, 1998). More structural studies are needed for better understanding of this process on the molecular level. This is especially true for archaebacteria which lie evolutionarily between bacteria and eukaryotes and for which no G-protein or GEF structures are known.

For structural studies of translation factors, archaebacteria present several advantages (Dennis, 1997). Archaebacterial translation displays a mixture of eukaryotic and bacterial features and their similarity to eukaryotes makes generalization to eukaryotic processes easier than in the case of studies on bacterial proteins. At the same time, archaeal systems are simpler than eukaryotic systems and more amenable to NMR and X-ray techniques. The genomes of a number of thermophilic archaebacteria have been completely or almost completely sequenced (e.g. *M. thermoautotrophicum*, *S. solfataricus*), so that their translational factors can be identified and cloned. These thermophilic translation factors are generally smaller, yet still show high degrees of homology with the eukaryotic factors. Thus, *M. thermoautotrophicum* EF-1β is 23% identical to the C-terminal portion of human eEF-1β, while the G-protein, *M. thermoautotrophicum* EF-1α, is over 50% identical to human eEF-1α. The translational machinery from these thermophilic organisms is more rugged and less susceptible to denaturation at temperatures typically used for NMR spectroscopy. We report here the structure of the archaeal translation elongation factor EF-1β determined by high resolution NMR spectroscopy.

Materials and methods

Sample preparation

Elongation factor aEF-1β from *M. thermoautotrophicum* (gene MTH1699) was subcloned into pET15b (Novagen, Inc., Madison, WI) and expressed in *E. coli* BL21 as an oligo-histidine (His-tag) fusion protein of 109 residues. Using a standard protocol, aEF-1β was purified by heat denaturation of endogenous *E. coli* proteins and affinity chromatography on Ni^{2+}-loaded chelating sepharose (Amersham Pharmacia Biotech, Piscataway, NJ). The efficiency of the heat denaturation step was improved by removing nucleic acids by passing the cell lysate over DEAE-sephacel in 0.5 M NaCl prior to heating. Isotopically labeled protein was prepared from cells grown on minimal M9 media containing ^{15}N ammonium chloride and/or ^{13}C glucose (Cambridge Isotopes Laboratory, Andover, MA). The N-terminal His-tag was cleaved from aEF-1β by treatment for 24 h at room temperature with thrombin (Amersham Pharmacia Biotech) at 1 unit per mg fusion protein. Benzamidine sepharose and Ni^{2+}-loaded chelating sepharose were used to remove thrombin and the His-tag peptide from aEF-1β. NMR samples were 2.0 to 3.0 mM in 50 mM sodium phosphate buffer, 0.15 M NaCl and 0.02% (w/v) sodium azide at pH 6.3. A 50 mM MES buffer, 0.15 M NaCl and 1 mM sodium azide at pH 6.3 was used for calcium binding studies.

NMR spectroscopy

NMR experiments (Bax and Grzesiek, 1993) were performed at 305 K on Bruker DRX500 and Varian UNITYplus 750 MHz spectrometers. Main-chain C^{α}, N, HN and side-chain C^{β} resonances were assigned using HNCACB and CBCA(CO)NH experiments (Grzesiek and Bax, 1992; Wittekind and Mueller, 1993). H^{α} resonance assignments and $^{3}J_{H^{N}-H^{\alpha}}$ coupling constants were obtained from an HNHA experiment (Kuboniwa et al., 1994). As described below, these

assignments were sufficient for the subsequent tertiary structure determination. The remaining backbone and side-chain signal assignments were obtained from ^{1}H-^{13}C HSQC, HCCHcosy, HNCO and two- and three-dimensional homo- and heteronuclear NOESY and TOCSY experiments. Nearly complete assignments were obtained for all the residues in aEF-1β. In the His-tag, the nine residues following the histidines were assigned; however, no backbone amide resonances for the six histidines and first four amino acids were detected. Chemical shifts were measured relative to internal sodium 2,2-dimethyl-2-silapentane-5-sulphonate (DSS) for ^{1}H and calculated assuming $\gamma^{15}N/\gamma^{1}H = 0.101329118$ and $\gamma^{13}C/\gamma^{1}H = 0.251449530$ (Wishart et al., 1995). NMR spectra were processed using GIFA (Pons et al., 1996) and XWINNMR software (Bruker Spectrospin) and analyzed with XEASY (Bartels et al., 1995).

Structure calculations

Structures were calculated using the ARIA module (Nilges et al., 1997) implemented in the program CNS (version 0.5) (Brunger et al., 1998). NOE restraints were obtained from ^{15}N- and ^{13}C-separated 3D NOESY experiments using mixing times of 100 ms and from a homonuclear 2D NOESY spectrum (110 ms mixing time) of aEF-1β. Distance constraints assigned by ARIA were calibrated according to NOE peak volumes. Manually assigned distance constraints were classified according to the peak intensities as strong (1.8–3.0 Å), medium (1.8–4.0 Å), and weak (1.8–5.0 Å). The φ torsion angles were derived from an HNHA experiment (Kuboniwa et al., 1994). The statistics for the structure calculations are shown in Table 1.

Results

Structure determination of aEF-1β was carried out using a sequential four-step protocol. First, backbone amide and carbon resonances were assigned using standard triple resonance experiments on doubly labeled protein (Figure 1). The protein secondary structure was analyzed using proton and carbon chemical shifts and $^{3}J_{H^N-H^\alpha}$ coupling constants (Spera and Bax, 1991; Wishart et al., 1991). This allowed the identification of four β-strands: amino acids 3–13 (strand β1), 36–43 (strand β2), 48–58 (strand β3) and 78–88 (strand β4). Two α-helices were also identified: amino acids 18–29 (α1) and 64–72 (α2) (Figure 2a). The results from NMR spectroscopy were in good agreement with computer-based secondary structure predictions.

In the second step, proton–deuterium exchange experiments were used to identify secondary structure elements in the protein core. Amide protons protected from solvent exchange were identified in series of ^{1}H-^{15}N HSQC spectra acquired after solvent exchange with D_2O. Beta-strands β1 and β3 contained the largest number of slowly exchanging amide protons (residues V5, A6, I8, K9 V10, M11, V49, A50, L51, V53, M54, V55, and V56). Strands β2 and β4 showed weaker protection with a pattern of protection of every second residue (e.g. L36, D40, E42) that is characteristic of the edge of a β-sheet. This information suggested the presence of a four-stranded β-sheet in the protein with strands β1 and β3 in the middle and strands β2 and β4 on the edges.

In the third step, the His-tag on aEF-1β was removed and ^{1}H-^{15}N correlation spectra from the tagged and untagged protein were compared (Figure 2b). A relatively small number of amide chemical shifts were affected by removal of the His-tag. The largest changes occurred in three regions: the N-terminus (in direct sequential proximity to the tag), the loop between strand β3 and helix α2 (amino acids V55 to E65) and the extreme C-terminus comprising amino acids R87, L88, and M89. Folding of the secondary structural elements to place these three regions together yielded the tertiary fold of aEF-1β. Specifically, strand β1 could be identified as antiparallel to strands β3 and β4. As an indirect consequence, the direction of strand β2 was identified and the order of strands in the antiparallel β-sheet was determined to be β4, β1, β3, and β2. The small sizes of the loop elements in aEF-1β meant that the orientation of helices α1 and α2 was also identified, as shown in Figure 2d.

Based on the natural twist of β-sheets, the α-helices of aEF-1β were predicted to lie behind the β-sheets. This resulted in a model of aEF-1β as a split β–α–β fold which regroups many RNA binding proteins, thioredoxin, and the proregions of microbial serine proteases (Orengo et al., 1999). Comparison of the model with protein structures available at the time revealed potential similarity between aEF-1β and domain V of another elongation factor, EF-G. In the particularly favorable case of aEF-1β, tertiary fold determination required less than one month of analysis following receipt of plasmid DNA expressing the protein.

In the fourth step of the structure determination, approximately 400 NOEs were used to calculate initial

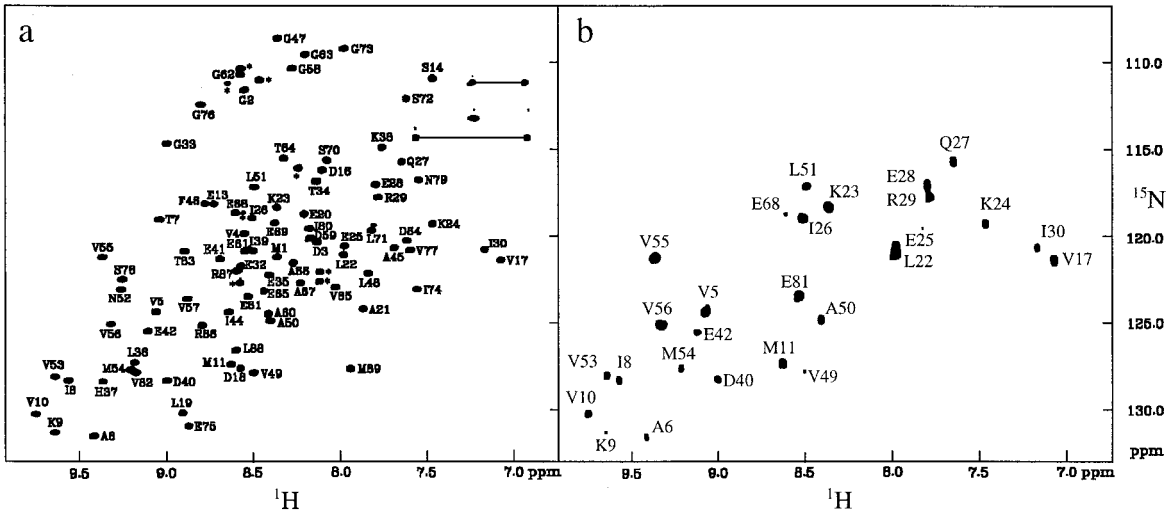

Figure 1. Assignments of amide resonances of the archaeal elongation factor aEF-1β and identification of residues in the protein core. (a) ^{1}H-^{15}N HSQC spectrum in H_2O solution, (b) spectrum acquired 15 min after transfer into D_2O. Only amide resonances protected from solvent exchange are visible in panel b.

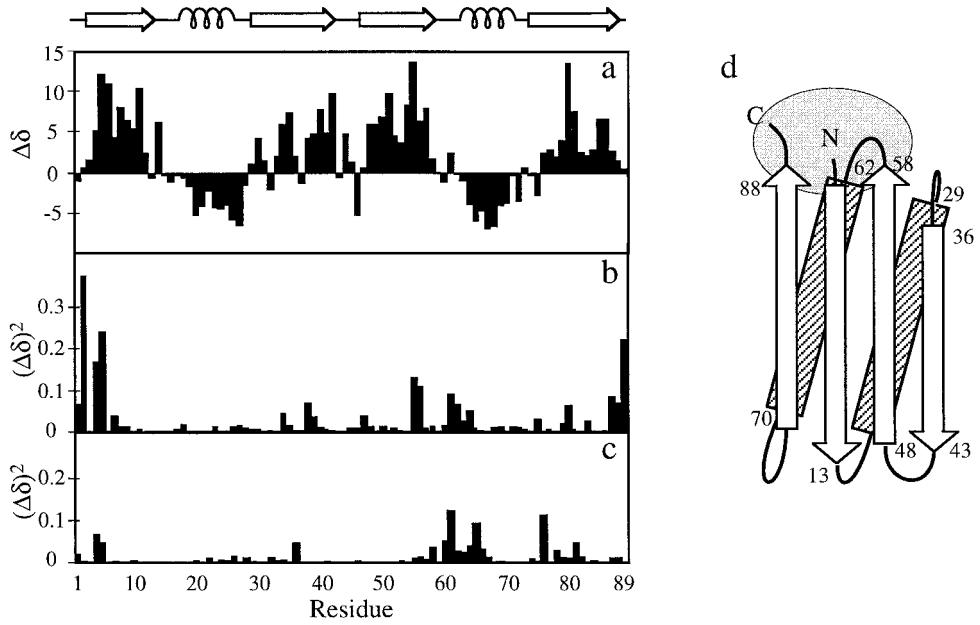

Figure 2. Secondary and tertiary fold of aEF-1β. (a) Identification of secondary structural elements from a summed secondary chemical shift (in ppm) calculated as $5{\cdot}\Delta\delta H^{\alpha} - \Delta\delta C^{\alpha} + \Delta\delta C^{\beta}$. The deduced secondary structure of two α-helices and four β-sheets is shown along the top. (b) Identification of residues in proximity to the N-terminal His-tag from the amide chemical shift perturbation calculated as $(5{\cdot}\Delta\delta H)^2 + (\Delta\delta N)^2$. (c) Identification of calcium binding site from the amide chemical shift perturbation. (d) Schematic diagram of the tertiary fold with the region affected by the His-tag highlighted in grey.

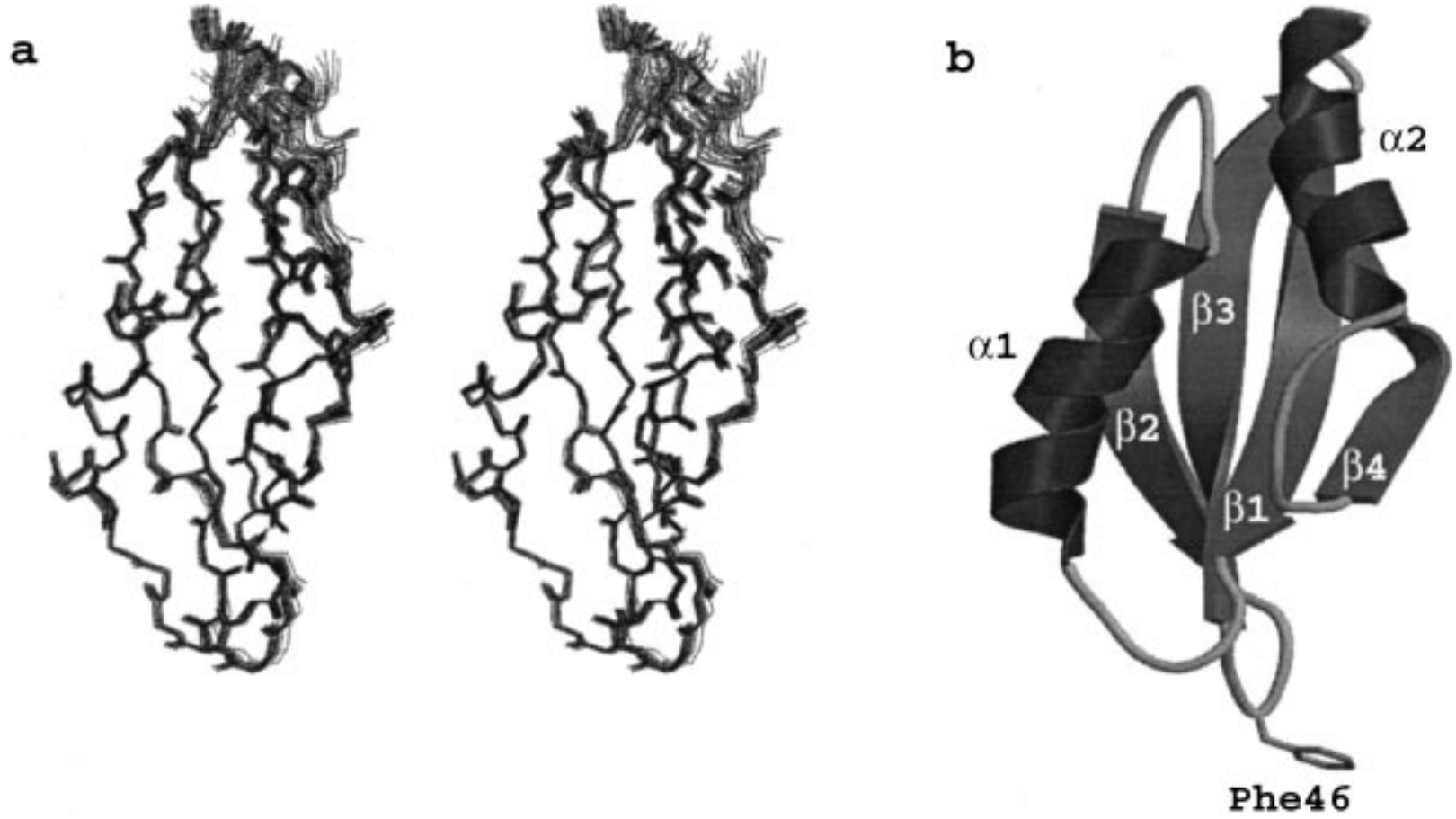

Figure 3. (a) Backbone overlay of the 30 lowest energy NMR structures of elongation factor aEF-1β from *Methanobacterium thermoautotrophicum*. (b) Ribbon representation of the average aEF-1β structure generated with MOLSCRIPT (Kraulis, 1991).

Table 1. Structure statistics of the archaeal translation elongation factor 1β

Restraints for structure calculations	
Total restraints used	1962
Total NOE restraints	1854
Intraresidue	680
Sequential (|i−j|=1)	453
Medium range (1<|i−j|≤4)	246
Long range (|i−j|>4)	475
Hydrogen bond restraints	26
Dihedral angle restraints	82
Statistics for structure calculations	<SA>[a]
Rmsd from idealized covalent geometry	
Bonds (Å)	0.0026±0.0001
Bond angles (°)	0.43±0.01
Dihedral angles (°)	0.39±0.04
Rmsd from experimental restraints[b]	
Distances (Å)	0.018±0.001
Final energies (kcal mol^{-1})	
E_{total}	249.3±12.5
E_{bonds}	9.1±0.8
E_{angles}	68.5±3.3
E_{vdW}[c]	100.2±4.7
E_{NOE}	31.9±4.6
Coordinate precision[d] (Å)	<SA> versus $<\overline{SA}>$
Rmsd of backbone atoms (N, Cα, C′) for residues 3–87	0.41±0.10
Rmsd of all heavy atoms for residues 3–87	1.20±0.11
Ramachandran plot statistics using PROCHECK[e] (%)	
Residues in most favoured regions	72
Residues in additional allowed regions	24
Residues in generously allowed regions	4

[a] <SA> refers to the ensemble of the 30 structures with lowest energy from 200 calculated structures.
[b] No distance restraint in any of the structures included in the ensemble was violated by more than 0.3 Å.
[c] Repel = 0.8 for the final step of calculations.
[d] Rmsd between the ensemble of structures <SA> and the average structure of the ensemble <SA>.
[e] Laskowski et al., 1996.

structures of aEF-1β. 2D NOESY, 3D ^{15}N-NOESY and 3D ^{13}C-NOESY spectra were used with ARIA to calibrate and assign previously unassigned cross peaks. The set of 1854 NOE distance restraints obtained after eight rounds of calculations was checked for errors and used to calculate the final set of structures (Figure 3A). The determined structure consists of four β-strands and two α-helices, βαββαβ, as shown in Figure 3B, and confirms the predicted fold. Both α-helices are located on one side of the domain and the antiparallel β-sheet is on another side. The residues Ile8, Val10, Val17, Leu22, Ile26, Ile30, Leu36, Leu51, Val53, Val55, Val57, Thr64, Ala67, Leu71, Ile74, Ile80, and Val82 form the hydrophobic core of the protein. The structure contains two distinguishing features: a distinct bulge at Glu81–Thr83 in the fourth β-strand and the presence of only one aromatic residue. This residue, Phe46, is located on the tip of the loop between strands β2 and β3 and points out into the solvent. The loop itself is unusually rich with hydrophobic residues (Ile44, Ala45, Phe46, Leu48).

In the course of these studies, aEF-1β was found to bind Ca^{2+}. The chemical shift changes upon calcium binding were used to map the binding site (Figure 2c).

The groove between strand β4 and helix α2 contains most of the residues with the biggest chemical shift changes. Since the absolute values of these changes are relatively small, the calcium binding does not appear to significantly alter the protein structure. The calcium-binding groove is a part of a surface that contains many negatively charged residues (Asp3, Glu32, Glu35, Asp59, Glu61, Glu65, Glu68, Glu69) and no positive residues. This negatively charged surface contributes to the binding of Ca^{2+}.

Discussion

The average protein domain size is estimated to be under 200 amino acids (Siddiqui and Barton, 1995; Burley et al., 1999; Thornton et al., 1999). Many of these domains with small loops and well-defined secondary structural elements should be amenable to rapid fold analysis by NMR. The cleavable His-tag provides a readily available tool for the chemical shift perturbation analysis that is the key to the method described here. For proteins with known ligands (e.g. a metal binding site), this analysis can be extended to include the analysis of local conformational changes induced by ligand binding. Similarly, fusion protein vectors with cleavable C-terminal extensions can be used to map residues near the protein's C-terminus. Our observation complements other NMR methods used for fold identification such as dipolar couplings (Annila et al., 1999). Identification of the protein fold can be used to generate suitable input structures for automated NOE assignment protocols (Nilges et al., 1997) and speeds the final structure determination. Since protein backbone assignments can be obtained more readily than high quality, comprehensive NOE restraints, these techniques should also allow fold analysis of proteins with solubility or stability problems.

During the course of this work, the structure of the homologous domain from human EF-1β was determined by NMR spectroscopy (Perez et al., 1999). Comparison of the two structures shows close similarity with a DALI Z-score of 6.7 (Holm and Sander, 1998). Along with identical architecture, both elongation factor proteins contain a similar bulge in the fourth β-strand and an exposed aromatic residue between the second and third β-strands. This structural conservation in EF-1β structures is striking and suggests that EF-1β from other eukaryotes and archaebacteria are very likely to have similar structures.

From comparative structural and sequence analysis of the EF-1β family of proteins, we can propose a mechanism for its function. Like its bacterial counterpart, EF-Ts, aEF-1β is a guanine nucleotide exchange factor that interacts with aEF-1α (the equivalent of EF-Tu). Examination of the EF-Tu/EF-Ts complex shows that Phe81 plays a critical role in the exchange activity of EF-Ts. In the complex, Phe81 is inserted into a hydrophobic patch of EF-Tu. This insertion shifts and disorders the Switch I and II helices, which destabilizes GDP binding (Kawashima et al., 1996; Wang et al., 1997). Phe81 is part of a conserved TDFV sequence motif found in all EF-Ts. Similarly in aEF-1β, the exposed residue, Phe46, is part of a conserved P+AFG+ motif found in archaebacterial and eucaryl EF-1β sequences. The second and last position of this motif are conserved as large hydrophobic residues, typically isoleucine or leucine, and the third position is often, but not always, alanine. Position 4 is invariably either phenylalanine or tyrosine. From our structure of aEF-1β, we propose that Phe46 acts as a lever to eject GDP from the G-protein, aEF-1α. A similar model has been proposed for the human protein, eEF-1β, by Perez et al. (1999). It appears that across all three kingdoms – archaea, eubacteria, and eukaryotes – EF-1β uses a common mechanism to effect nucleotide exchange.

The calcium binding is a novel feature for nucleotide exchange factors. This metal binding seems to be quite specific since several other metals tested (e.g. Mg^{2+}) did not bind to aEF-1β. The calcium ions here may play a purely structural role in stabilizing the protein (for examples, see Vyas et al., 1989; Chen et al., 1999; Dzwolak et al., 1999; Smith et al., 1999). Alternatively, calcium may participate functionally by affecting either aEF-1β activity towards aEF-1α or binding to other protein factors. Future studies will test these hypotheses by site-directed mutagenesis of aEF-1β and finer mapping of the residues that interact with calcium by NMR spectroscopy.

Acknowledgements

This project is part of the Canadian Structural Genomics Initiative (Cheryl Arrowsmith and Aled Edwards, Ontario Cancer Institute and the University of Toronto, Toronto, ON, Canada). The PDB accession number for the coordinates is 1D5K. ^{1}H, ^{15}N and ^{13}C signal assignments for residues 1 to 89 of aEF-1β in the His-tag fusion protein have been deposited

in the BioMagResBank (http://www.bmrb.wisc.edu) under accession number 4385. We thank the Pacific Northwest National Laboratory for access to the Environmental Molecular Sciences Laboratory High Field Magnetic Resonance Facility. This study was supported by a grant from the Medical Research Council of Canada to K.G. NRC publication no. 42950.

References

Annila, A., Aitio, H., Thulin, E. and Drakenberg, T. (1999) *J. Biomol. NMR*, **14**, 223–230.

Arcari, P., Gallo, M., Ianniciello, G., Dello, R.A. and Bocchini, V. (1994) *Biochim. Biophys. Acta*, **1217**, 333–337.

Arcari, P., Raimo, G., Ianniciello, G., Gallo, M. and Bocchini, V. (1995) *Biochim. Biophys. Acta*, **1263**, 86–88.

Bartels, C., Xia, T.-H., Billeter, M., Güntert, P. and Wüthrich, K. (1995) *J. Biomol. NMR*, **6**, 1–10.

Bax, A. and Grzesiek, S. (1993) *Acc. Chem. Res.*, **26**, 131–138.

Berman, H.M., Westbrook, J., Feng, Z., Gilliland, G., Bhat, T.N., Weissig, H., Shindyalov, I.N. and Bourne, P.E. (2000) *Nucleic Acids Res.*, **28**, 235–242.

Boriack, S.P., Margarit, S.M., Bar, S.D. and Kuriyan, J. (1998) *Nature*, **394**, 337–343.

Brenner, S.E. and Levitt, M. (2000) *Protein Sci.*, **9**, 197–200.

Brunger, A.T., Adams, P.D., Clore, G.M., DeLano, W.L., Gros, P., Grosse, K.R., Jiang, J.S., Kuszewski, J., Nilges, M., Pannu, N.S., Read, R.J., Rice, L.M., Simonson, T. and Warren, G.L. (1998) *Acta Crystallogr. D (Biol. Crystallogr.)*, **54**, 905–921.

Burley, S.K., Almo, S.C., Bonanno, J.B., Capel, M., Chance, M.R., Gaasterland, T., Lin, D., Sali, A., Studier, F.W. and Swaminathan, S. (1999) *Nat. Genet.*, **23**, 151–157.

Chen, B., Costantino, H.R., Liu, J., Hsu, C.C. and Shire, S.J. (1999) *J. Pharm. Sci.*, **88**, 477–482.

Cherfils, J., Menetrey, J., Mathieu, M., Le, B.G., Robineau, S., Beraud, D.S., Antonny, B. and Chardin, P. (1998) *Nature*, **392**, 101–105.

Dennis, P.P. (1997) *Cell*, **89**, 1007–1010.

Dzwolak, W., Kato, M., Shimizu, A. and Taniguchi, Y. (1999) *Biochim. Biophys. Acta*, **1433**, 45–55.

Grzesiek, S. and Bax, A. (1992) *J. Am. Chem. Soc.*, **114**, 6291–6293.

Holm, L. and Sander, C. (1998) *Nucleic Acids Res.*, **26**, 316–319.

Jiang, Y., Nock, S., Nesper, M., Sprinzl, M. and Sigler, P.B. (1996) *Biochemistry*, **35**, 10269–10278.

Kawashima, T., Berthet, C.C., Wulff, M., Cusack, S. and Leberman, R. (1996) *Nature*, **379**, 511–518.

Kraulis, P.J. (1991) *J. Appl. Crystallogr.*, **24**, 946–950.

Kuboniwa, H., Grzesiek, S., Delaglio, F. and Bax, A. (1994) *J. Biomol. NMR*, **4**, 871–878.

Laskowski, R.A., Rullmann, J.A., MacArthur, M.W., Kaptein, R. and Thornton, J.M. (1996) *J. Biomol. NMR*, **8**, 477–486.

Masullo, M., De Vendittis, E. and Bocchini, V. (1994) *J. Biol. Chem.*, **269**, 20376–20379.

Nilges, M., Macias, M.J., O'Donoghue, S.I. and Oschkinat, H. (1997) *J. Mol. Biol.*, **269**, 408–422.

Orengo, C.A., Pearl, F.M., Bray, J.E., Todd, A.E., Martin, A.C., Lo, C.L. and Thornton, J.M. (1999) *Nucleic Acids Res.*, **27**, 275–279.

Perez, J.M., Siegal, G., Kriek, J., Hard, K., Dijk, J., Canters, G.W. and Moller, W. (1999) *Structure*, **7**, 217–226.

Pons, J.-L., Malliavin, T.E. and Delsuc, M.A. (1996) *J. Biomol. NMR*, **8**, 445–452.

Raimo, G., Masullo, M., Savino, G., Scarano, G., Ianniciello, G., Parente, A. and Bocchini, V. (1996) *Biochim. Biophys. Acta*, **1293**, 106–112.

Sali, A. (1998) *Nat. Struct. Biol.*, **5**, 1029–1032.

Siddiqui, A.S. and Barton, G.J. (1995) *Protein Sci.*, **4**, 872–884.

Smith, C.A., Toogood, H.S., Baker, H.M., Daniel, R.M. and Baker, E.N. (1999) *J. Mol. Biol.*, **294**, 1027–1040.

Spera, S. and Bax, A. (1991) *J. Am. Chem. Soc.*, **113**, 5490–5492.

Sprang, S.R. and Coleman, D.E. (1998) *Cell*, **95**, 155–158.

Thornton, J.M., Orengo, C.A., Todd, A.E. and Pearl, F.M. (1999) *J. Mol. Biol.*, **293**, 333–342.

Vyas, M.N., Jacobson, B.L. and Quiocho, F.A. (1989) *J. Biol. Chem.*, **264**, 20817–20821.

Wang, Y., Jiang, Y., Meyering, V.M., Sprinzl, M. and Sigler, P.B. (1997) *Nat. Struct. Biol.*, **4**, 650–656.

Wishart, D.S., Bigam, C.G., Yao, J., Abildgaard, F., Dyson, H.J., Oldfield, E., Markley, J.L. and Sykes, B.D. (1995) *J. Biomol. NMR*, **6**, 135–140.

Wishart, D.S., Sykes, B.D. and Richards, F.M. (1991) *FEBS Lett.*, **293**, 72–80.

Wittekind, M. and Mueller, L. (1993) *J. Magn. Reson.*, **B101**, 201–205.